Conserved long noncoding RNA *TILAM* promotes liver fibrosis through interaction with PML in HSCs

Cheng Sun[*], Chan Zhou[*], Kaveh Daneshvar[*], Amel Ben Saad, Arcadia J. Kratkiewicz, Benjamin J. Toles, Nahid Arghiani, Anja Hess, Jennifer Y. Chen, Joshua V. Pondick, Samuel R. York, Wenyang Li, Sean Moran, Stefan Gentile, Raza Ur Rahman, Zixiu Li, Peng Zhou, Robert Sparks, Tim Habboub, Byeong-Moo Kim, Michael Y. Choi, Silvia Affo, Robert F. Schwabe, Yury V. Popov, and Alan C. Mullen[†]

* These authors contributed equally.

[†]Corresponding author. Email: alan.mullen@umassmed.edu

Table of Contents

Supplemental Materials and Methods

Animal studies

All mouse experiments were approved by the IACUC of the Massachusetts General Hospital (2017000074) or Columbia University (AC-AAAF7452). For the carbon tetrachloride (CCl_4) model of fibrosis, mice received either 40% CCl_4 diluted in olive oil or olive oil control by oral gavage (100 µl total volume) three times a week for four weeks(1). For the choline-deficient, L-amino acid-defined, high-fat diet (CDA-HFD) model, mice were fed CDA-HFD chow consisting of 60% kcal fat and 0.1% methionine or control chow for twelve weeks(2,3). HSCs were sorted from *Lrat-Cre* mice crossed with ZsGreen *Cre* reporter mice (*R26R*^{zsGreen}, Jackson Laboratory) as described(4,5) either before or after receiving CCl_4 by intraperitoneal injections (0.5 ml/g, dissolved in corn oil at a ratio of 1:3) three times a week for four weeks. All animals received humane care according to the criteria outlined in the "Guide for the Care and Use of Laboratory Animals" prepared by the National Academy of Sciences and published by the National Institutes of Health (NIH publication 86-23 revised 1985).

Generation of Tilam mouse

Tilam$^{gfp/gfp}$ mice were generated by injecting a cocktail of crRNA+tracrRNA, Cas9 protein and donor DNA into pronuclei of E0.5 C57BL/6 embryos. Two crRNAs targeting *Tilam* were mixed 1:1 for injection (Supplemental Dataset 1). Donor DNA consisted of a plasmid containing GFP and polyA cDNA sequence inserted into exon 1 of *Tilam* (between nt 55 and 56), with 4 kb of genomic homology sequence flanking each side of the insertion site. Post-injection embryos were re-implanted into recipient CD1 pseudo-pregnant females and allowed to develop to term. Pups were screened by genomic PCR to identify founders, initially using a 5' primer recognizing a sequence

outside the 4 kb homology arm and 3' primer recognizing a sequence in the GFP cDNA (Supplemental Dataset 1). Founders were back-crossed to C57BL/6 mice (Charles River) to confirm germline transmission and backcrossed for six generations to wild-type C57BL/6 mice before *in vivo* fibrosis experiments were performed. Genomic DNA was then isolated from mice after the backcrosses, and the locus was amplified and sequenced to confirm that the *GFP-polyA* cassette was inserted between nucleotides 55 and 56 of exon 1 (Supplemental Figure 4C). Subsequent genotyping was performed with primers described in Supplemental Dataset 1 and through probe sets designed by Transnetyx. Studies were initiated on age and sex-matched wild-type and *Tilam*$^{gfp/gfp}$ mice on the same C57BL/6 background at 8-10 weeks of age.

Experimental mouse cohort

Both male and female mice were evaluated separately to analyze the phenotype in wild-type and *Tilam*$^{gfp/gfp}$ mice. Figure legends indicate the sample size for each result, represented by individual data points. Animal numbers for sample harvest are: wild-type = 135, *Tilam*$^{gfp/gfp}$ = 127. Age and sex-matched control wild-type mice of the same C57BL/6 background (Charles River) were purchased and were co-housed for two weeks prior to experiments. The mice were fed with the LabDiet Prolab IsoPro RMH 3000, 5P76 and housed in Allentown PIV cage on sani chip hardwood bedding and given carefresh as a nesting material.

Cell culture

Primary human HSCs were purchased from Lonza, and LX-2 cells were a gift from Scott Friedman. Cells were cultured as described previously for HSCs(6). Details for each individual donor are listed below. Primary mouse HSCs were isolated and cultured as previously

described(7). HEK-293 cells were obtained from ATCC (CRL-1573) and cultured in DMEM supplemented with 10% fetal calf serum and 1% Penicillin/Streptomycin. For HSC gene expression analysis by qRT-PCR in the presence of TGF-β1 or TGF-β2 (R&D Systems), HSCs were cultured in DMEM with 0.2% BSA for 2 days and then treated for 16 hr. For IF experiments, HSCs were cultured in DMEM with 0.2% BSA for 1 day before treatment for 6 hr.

Donor	Vendor ID	Age	Gender	Race	BMI
1	Lonza, HUCNP, ID: 4105	45	M	Caucasian	24.2
2	Lonza, HUCNP, ID: 4270	35	M	Caucasian	42.1
3	Lonza, HUCNP, ID: 4119	30	F	African American	33.2
4	Lonza, HUCLS, ID: 201951	28	M	Caucasian	24.4
5	Lonza, HUCLS, ID: 182821	24	F	African American	48.8

Expression analysis of TILAM in patients with metabolic dysfunction-associated steatotic liver disease.

RNA-seq data were analyzed from 206 patients diagnosed with metabolic dysfunction-associated steatotic liver disease (MASLD/NAFLD) from GSE135251(9). For gene quantification, we employed the GENCODE (v42) GTF file and FeatureCounts(10) to calculate locus-specific read counts. These counts were normalized to Fragments Per Kilobase of transcript per Million (FPKM), accounting for both gene exon lengths and sample-specific unique-mapped read counts. We quantified *TILAM* (including all isoforms from our prior study(8) and those annotated in GENCODE v42) and *COL1A1* FPKM values between patients as stratified in the dataset: 51 patients with metabolic dysfunction-associated steatosis without steatohepatitis (MAFLD), 24 patients with metabolic dysfunction-associated steatohepatitis (MASH) and F0-F1 fibrosis, 53 patients with MASH and F2 fibrosis, 53 patients with MASH and F2 fibrosis, and 14 patients with MASH and F4 fibrosis. Statistical significance was assessed using the Wilcoxon-Mann-Whitney test.

Human embryonic stem cell (hESC) culture and liver organoid differentiation.

H1 hESCs (WA01, NIH registration number 0043) were obtained from WiCell, and ESCRO approval for their use was received from UMass Chan Medical School and Massachusetts General Hospital. hESCs were cultured, and genome editing with homology directed repair (HDR) was performed as previously described(11). In brief, hESCs were co-transfected with Cas9 protein-crRNA-tracrRNA complex (Supplemental Table 7) and homology vector followed by puromycin selection. Individual puromycin-resistant colonies were selected and expanded. Genomic sequencing was then performed to confirm homozygous insertion.

hESCs were differentiated into liver organoids as previously described(12,13). In brief, cells were differentiated to definitive endoderm then to foregut spheroids. On day 7 of differentiation, cells were embedded in Matrigel (Corning, 354230) and treated for 4 days with retinoic acid (Tocris,

0695) before switching to Hepatocyte Culture Medium (Lonza, CC-3198). On day 21, liver organoids were extracted from Matrigel and cultured on an orbital shaker(13). Where indicated, isolated liver organoids were treated with TGF-β1 (10 ng/mL) and FGF-1 (at indicated dose) for 4 days to induce fibrosis. LNAs were added to culture media (500 nM) for 48 hr to deplete *TILAM* expression.

For immunofluorescent analysis, HLOs were collected, fixed with 4% paraformaldehyde (PFA) and then permeabilized using 0.1% Triton. See Supplemental Dataset 2 for antibodies. DAPI (1:10000) was used to stain nuclei (62248, Thermofisher). The stained HLOs were visualized and imaged with the Leica DMi8 automated Microscope (Leica Systems) using the 10x objective.

Delivery of short interfering (si) RNAs and locked nucleic acids (LNAs)

Human HSCs were reverse transfected with siRNAs(6), and human HSCs were transduced with LNAs with reverse transfection or nucleofection, as indicated. Reverse transfection was performed using Dharmafect-1 transfection reagent (Horizon Discovery, cat# T-2001) according to the manufacturer's instructions. For 12-well plates, 60μL of 3μM siRNAs or LNAs were added to 180 μL Opti-MEM (Gibco, cat# 31985070) for the final concentration of 150nM and then mixed with diluted Dharmafect-1 in Opti-MEM (2.4 μL Dharmafect-1 in 237.6 μL Opti-MEM). After 30 min, HSCs resuspended in transfection medium (DMEM supplemented with 16% FBS) were seeded in wells containing the siRNA or LNA/Dharmafect-1 mixture at ~70,000 cells/mL in 720 μL/well. Transfection in other plate formats were scaled up or down based on surface area. Cells were incubated with siRNAs or LNAs and transfection reagents for 72 hr before analysis. The siRNAs were purchased from Horizon Discovery. and the LNAs were purchased from Qiagen (Supplemental Dataset 1).

Nucleofection was performed for human HSCs (Figure 1D) and murine HSCs (Figure 4B). HSCs

($0.5x10^6$) were resuspended in 1M nucleofection buffer (5 mM KCl, 15 mM MgCl2, 120 mM Na2HPO4/NaH2PO4 pH 7.2, 50 mM Mannitol) and transfected with 200 nM LNA/ASO in a Nucleofector 4D (Lonza). HSCs were harvested after 48 hr of treatment. The ASOs against murine *Tilam* were purchased from Integrated DNA Technologies (Supplemental Dataset 1)

qRT-PCR analysis

RNA samples were extracted using Qiagen RNeasy Mini Kit (74104). Using 500 ng total RNA as input, reverse transcription was performed with the iScript gDNA Clear cDNA Synthesis Kit (BIO-RAD, 1725035) according to manufacturer's instructions. *TILAM*/*Tilam* expression was quantified in human and murine HSCs using SYBR Green Universal Master Mix (Applied Biosystems, cat# 4309155) with primers listed in Supplemental Dataset 1 with the exception of Supplemental Figure 2D and 2E, which used TaqMan Universal PCR Master Mix (Applied Biosystems, cat# 4305719) and TaqMan Real-time PCR Assays (ThermoFisher Scientific). SYBR Universal Master Mix with primers listed in Supplemental Dataset 1 were also used for Figure 2B and Supplemental Figure 7A. All other qRT-PCR experiments were performed with TaqMan Universal PCR Master Mix and TaqMan Real-time PCR Assays, and gene-specific Real-time PCR Assays used in this study are listed in Supplemental Dataset 1. *GAPDH* was used as an endogenous control for all experiments unless otherwise stated.

Immunofluorescent staining and single molecule RNA fluorescent in situ hybridization (smFISH)

For immunofluorescence in Figure 7, HSCs were cultured on coverslips and washed with PBS at least three times and fixed in 4% paraformaldehyde (PFA) in PBS for 15 min at room temperature. Cells were then permeabilized with 0.05% Triton X-100 in PBS and blocked in blocking solution

(0.1% BSA in PBS) for 1 hr. Then, coverslips were subjected to incubation with primary antibodies in the blocking solution overnight at 4 °C. Coverslips were then washed three times with PBS and then treated with secondary antibodies in the blocking solution for 1 hr at room temperature. Cells were then washed three time with PBS. Cells were stained with DAPI for 15 min before washinsg with PBS. The coverslips were mounted and visualized for fluorescence on a Leica Thunder imager (LEICA DMi8). See Supplemental Dataset 2 for antibodies.

For Supplemental Figure 7F, Immunofluorescent staining was performed as previously described(11) following the sequential immunostaining and single-molecule RNA-FISH protocol for HSCs cultured on glass coverslips. Cells were fixed in 3.7% formaldehyde in DPBS and permeabilized in 1% Triton X-100. Cells were stained with Hoechst and mounted onto slides. Slides were imaged on a StellarVision inverted microscope (Optical Biosystems, model SV20HT) using a Nikon CFI S Plan Fluor ELWD 0.45NA 20XC air objective.

Single molecule RNA FISH was performed as previously described(14). Custom Stellaris® FISH probes (Biosearch Technologies) were designed against *TILAM* and *PDGRFB* using the Stellaris® FISH Probe Designer (www.biosearchtech.com/stellarisdesigner, Supplemental Dataset 3). HSCs were cultured on glass coverslips before fixation and overnight hybridization with Stellaris FISH probe sets labeled with Quasar570 or Quasar670, following the manufacturer's instructions. (www.biosearchtech.com/stellarisprotocols). Nuclei were defined by Hoechst staining. Imaging was performed with a Nikon 80i upright fluorescence microscope with Hamamatsu Orca CCD camera.

Formaldehyde-assisted isolation of regulatory elements (FAIRE)

FAIRE was performed as previously described(14), and primers are described in Supplemental Dataset 1.

Rapid amplification of cDNA ends (RACE)

Total RNA was isolated from human and murine HSCs. RNA was isolated by the microFast Track 2.0 kit (Life Technologies). The GeneRacer 2.0 kit (Life Technologies) was used to determine the 5' and 3' ends of the lncRNA transcripts. Nested 5' and 3' RT-PCR was performed in human HSCs and a single round of 5' and 3' RT-PCR was performed in murine HCS. Primers are listed in Supplemental Dataset 1.

Nuclear and cytoplasmic fractionation

Nuclear and cytoplasmic fractionation was performed as previously described(14). Primers used for qRT-PCR are listed in Supplemental Dataset 1.

RNA-Seq

Human HSCs from donor 4 (Lonza, HUCLS, ID: 201951) were transfected with NTC si5 (control), *PML* si17, LNA Ctrl (control), and *TILAM* LNA1 in triplicate. Cells were harvested, and RNA was extracted using Qiagen RNeasy Mini Kit (74104). Analyzed samples showed an RNA quality number (RQN) greater than 9 (Agilent 4200 TapeStation System). PolyA-selection and stranded library preparation (NEB Directional Ultra II RNA library preparation kit) was performed prior to 150 nt paired-end sequencing on a HiSeq4000. Murine HSC libraries were created from sorted HSCs and prepared with the Illumina Truseq mRNA Stranded Prep Kit prior to 100 nt paired-end sequencing on a HiSeq2500.

RNA-seq analysis and differential gene expression

For analysis of human HSC data, reads were quality assessed using the FASTQC (v 0.11.9) and aligned to the human reference genome (GRCh38_release_37) from GENCODE with Star aligner (v2.7.10a) using RSEM (v1.3.3) with default parameters. First, the human reference genome was indexed using the GENCODE annotations (gencode.vGRCh38_release_43) with rsem-prepare-reference from RSEM software. Next, rsem-calculate-expression was used to align the reads and quantify gene abundance. The output of rsem-calculate-expression gives separately the read count and transcripts per million (TPM) value for each gene. Differential expression analysis was performed using gene read counts with DESeq2 package (v 1.38.3) to produce LFC values and corresponding p-values (FDR) applying a Benjamini–Hochberg correction for multiple testing, with a minimum of 5 reads required for a differentially-expressed gene. The heatmap was created using normalized gene count values from Deseq2, using R gplots package heatmap.2 function with row scaling. GO analysis was performed and visualized with WebGestalt(15). Gene expression across cell types and tissues for human and mouse samples were performed as previously described(8,14), except that for Supplemental Figure 1*C*, the original FPKM values were converted into transformed Z-scores so that the values for *Col1a1* and *Tllam* could be compared on the same plot.

Identification of orthologous long noncoding RNAs between humans and mice

RNA-seq data from murine HSCs were mapped to the mouse reference genome (mm10), and *ab initio* assembly was performed as previously described(8). To identify orthologous lncRNAs between humans and mice, we integrated three distinct methods: synteny analysis, whole genome alignment (WGA), and sequence similarity (SS).

(1) Synteny: An lncRNA was considered as synteny-orthologous between human and mouse HSCs if it met the following criteria: a) it was expressed in both human and mouse HSCs, b) it was located within 10 kb of the same coding gene (as defined by genes in the human and mouse genomes with the same name, and c) it exhibited consistent relative strand information corresponding to the coding gene.

(2) Whole Genome Alignment (WGA): Orthologous lncRNAs identified via WGA were located in the same region of the aligned genomes of humans and mice. We obtained whole-genome alignment chains between the human genome (hg19) and mouse genome (mm10) from the UCSC Genome Browser. We then assigned a location for each lncRNA into 2,000 bins within these aligned chains in both species.

(3) Sequence Similarity (SS): An lncRNA was deemed orthologous via sequence similarity if its human and mouse transcripts showed significant similarity, defined by an e-value of less than 1e-5 in a bi-directional search. The sequence alignment search was performed using the BLAST algorithm with the following parameters: blastall -p blastn -i query_seq.fa -d target_seq.fa -e 0.00001 -m 0 -W 8.

Single-cell RNA sequencing analysis

Single-cell RNA-seq data from olive oil control and CCl_4-treated mice were obtained from GSE171904(16). Using the experimentally confirmed murine *Tilam* transcript sequence (Supplemental Figure 3D), we identified its genomic coordinates as two exons on chromosome 11 (chr11:94933400-94933501 and chr11:94928436-94929302, mm10 reference genome, minus strand) via BLAT sequence alignment (17). These coordinates were incorporated into the mm10 genome annotation file, and a custom Cell Ranger reference was created using the 'mkref' command. CellRanger (version 7.0.1; 10x Genomics) was used to generate expression matrices with default parameters, which were subsequently merged and analyzed in R using the Seurat

package (18). Only cells expressing more than 200 genes, and only genes present in at least three cells were retained. Data were log-normalized, and cell type relationships and UMAP coordinates were derived from the RDS files accompanying the GSE171904 dataset. UMAP plots were created using the "seaborn" Python package.

Hepatic hydroxyproline

To quantify collagen level, liver samples were isolated from the same region of the left liver lobe and analyzed as described(19). Isolated samples were homogenized and processed to evaluate hydroxyproline concentration using hydroxyproline assay kits following manufacturer's instructions (Sigma-Aldrich, MAK008).

Collagen proportionate area (CPA)

CPA was measured as described previously(20). Liver samples were fixed in 4% PFA. Pico-Sirius red staining was performed using the left liver lobe from PFA-fixed paraffin embedded sections. Whole sections were scanned and loaded into ImageJ to calculate the ratio of collagen positive area against the total parenchyma area and expressed as a percentage.

Immunohistochemistry

Immunohistochemistry (IHC) was conducted on paraffin sectioned samples. For paraffin-embedded sectioning, livers were fixed in 4% PFA at 4°C. After dehydration through graded ethanol and paraffin embedment, samples were sectioned at 5-μm. Standard

immunofluorescence procedure with antigen recovery was carried out. Antibodies are listed in Supplemental Dataset 2.

Linear model analysis of results from male and female mice

Separate linear regression models were constructed to investigate the gender-specific effects of *Tilam*$^{gfp/gfp}$ mice based on hydroxyproline levels in the CCl_4 and CDA-HFD experiments. The linear regression models were fitted using the lm function in R. To perform this analysis, sample numbers were equalized by using the k-nearest neighbors (KNN) imputation with the impute.knn function in the impute package to fill in values so each condition had equal number of samples for the linear regression model. Separate imputations were performed for the CCl_4 and HFD.

Western blot analysis, nuclear lysate production, and co-immunoprecipitation

For analysis of whole cell lysates (Figure 7A, Supplemental Figure 7D), pelleted cells were lysed with RIPA buffer (Thermo Scientific, 89900) supplemented with protease inhibitors (Thermo Scientific, 87786). Cell lysates were centrifuged to remove debris. Protein concentrations were measured using Pierce BCA Protein Assay Kit (Thermo Scientific, 23227). LDS Sample Buffer (Invitrogen, B0007) and Sample Reducing Agent (Invitrogen, B0009) were added to cell lysate, and the sample mixture was boiled for 10 min before loading. 4% to 12% Bis-Tris gels (Invitrogen, NW04120BOX) were used for electrophoresis followed by transfer using iBlot 2 Dry Blotting System (Invitrogen, IB21002S). Membranes were blocked with 1% BSA (Thermo Scientific, 37520) at room temperature for 1 hr and incubated overnight with primary antibody at 4°C. Membranes were washed three times with Tris Buffered Saline-Tween (TBST) buffer (Boston BioProducts, IBB-181–6), incubated with secondary antibody for another 1 hr, washed three times

with TBST buffer, and then incubated with SuperSignal West Pico PLUS chemiluminescent substrates (Thermo Scientific, 34580) for 5 min before scanning with a LI-COR Odyssey M imaging system. Antibodies are listed in Supplemental Dataset 2.

For isolation of nuclear lysates (Figure 7G, Supplemental Figure 7C and D), nuclear isolation was performed as described previously (11). HSCs were washed with PBS, scraped on ice, and transferred to 15 ml conical tubes. The cells were pelted by cold centrifugation at 400*g*. After washing 2 times with cold PBS, cell pellets were suspended in hypotonic buffer (20 mM Tris-HCL pH 7.4, 10 mM NaCl, 3mM $MgCl_2$) and incubated on ice for 15 min. Ten percent NP40 was then added to the pellets and vortexed at the highest setting. Nuclear pellets were collected after centrifugation at 845*g* at 4 °C. Lysates were then prepared for gel electrophoresis and protein quantification as described in the first paragraph of this section. Antibodies are listed in Supplemental Dataset 2.

To perform Co-IP (Figure 7G), the pellets containing nuclei were lysed in a lysis/wash buffer (50 mM Tris-HCL pH 7.5, 150 mM NaCl, 1 mM EDTA, 1% Triton X-100 and 1× Halt protease inhibitor). Following centrifugation at 16,000*g* for 20 min, supernatants were incubated with PML antibody or normal rabbit IgG overnight at 4 °C with gentle rotation. Then, Dynabeads Protein G (Thermo Fisher Scientific, 10003D) were washed once in lysis/wash buffer and incubated with lysate-antibody conjugate mixture at 4 °C with rotation for 1 hr. After collecting the beads by placing the tubes on a magnetic rack and washing 3 times with lysis/wash buffer, samples were eluted and treated as described in the first paragraph of this section for gel electrophoresis and analysis. Antibodies are listed in Supplemental Dataset 2.

Lentiviral Transduction of HSCs

Lentivirus was produced in HEK-293T cells with pMD2.G (Addgene plasmid # 12259) and psPAX2 (Addgene plasmid # 12260) using X-tremeGENE 9 transfection reagent as previously described(6) to package lentivirus expression *TILAM*-apt or *SCRM*-apt.

Mass spectrometry and analysis

LX-2 cells were infected with lentivirus expressing *TILAM-apt* or *SCRM-apt* and selected with puromycin. Confluent cells were rinsed with DPBS and exposed to 400 mJ/cm^2 of energy on ice using a UV cross-linker (Stratalinker). UV cross-linked cells were lysed (150 mM KCl, 25 mM Tris-HCl pH 7.4, 5 mM EDTA, 5 mM MgCl2, 1% NP-40, 0.5 mM DTT, Roche mini-tablet protease inhibitor, 100 U/mL RNAseOUT), and debris was removed by centrifugation at 16000*g*. The resulting lysate was further treated with 50 µL of Avidin Agarose beads (Thermo Fisher, 20219) to clear biotin from the lysates. The cleared lysate was then incubated with 150 µL of Streptavidin C Dynabeads (Thermo Fisher) on a rocker at 4°C for 4 hr. The beads were collected using a magnet and washed three times with a wash buffer similar to the lysis buffer, except for an increased KCl concentration of 350 mM. To release the proteins, the beads were incubated with RNase A and resuspended in 2X LDS sample buffer. Lysates were resolved on a polyacrylamide gel, and segments ranging from 30 to 350 kDa were excised for subsequent mass spectrometry analysis. The resulting proteomic data were analyzed using Crapome proteomic analysis (https://reprint-apms.org/) with a threshold of >90% confidence and a greater than four-fold enrichment over controls.

A

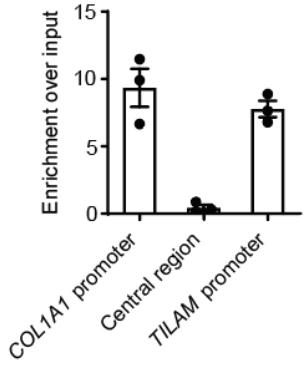

B

hTILAM

AGTACTGGTCAGGTATTCCATAGAATGTCCTACTGTTAGCTTTCAGAACTTCTGGAGGCCTGGGATT
CTGGGGGAAGGAGTTATACTCAGTGGTGGCCATAGAGAGTTGGTGACTGCCTTTGAGAGGAGAAT
GGTTGTGATCCTTTTGCCGAGAACTCACCCAGAGGACTTATACCTTGGTGACAGCAGAAGGACTCA
AGTTAGAAGGCCAGGGCCCTTAAAGGGAGGGGACGATTCGAGATTAGAAAACTGAGGCCCAGAGA
AGGAAAGTAGCTGCCAGAGGTCACACAGCTAGGATTGAGGGATCAGAGACTGCTGCAGCCCAGAT
GCCTTCGCAGCCATGGCCTGGCCCATCCAACCCGCTGACCTCATTCCCAGCTCCCCTCTCTTGCAA
GCTCCCCCCTTGCCTGCCACGTAGACTGGAGGCTTAGCTGCATCTTCGCTGGAGGGAGGAAGAGC
AGAACACAGAGGCCCTGAGCCCAGAGCTCTGCTGGGTCAGACTGGCCTGGGGAGAGCAGCTGTG
TTCCTCCAGCGCCCCCCAAGACCAGGCTGGGCCTCAGTTTGCCCTCCTCAAACCTCCTCAAACCTG
AGGCCCAGAAGGTGGAGGGGACAGAGGTCATGGGAGAAGCATGACAATGAAGTGGGTTGGAGTG
GGCGAGAATCACGTGGGGGCTCTGAGGTCATTGTAGCCATCCCCCTGCCTCCTCAGGGCAGGAG
GGTGCTAGGATCAGACCCAGAAAGGGACAGGGGCAGGACATTCCTCCTCTTTTCAAGCATTCACAA
GAAGCAGAGTTCCATGGTGGTCTAGGAGGGGGTCCTTTGTAAGATCTAGTCTTCCTCCTTCTGCTG
TGTGAGGACCACAGTATGTGGCTAGGACGAGGTGGGCGAGTTCCTCCTCCCCCACAAGCTGGCAC
ATGTGGATATTGGCTCTGTTTTGCCTTTGACCCCTAGTGAAAGAAAATACTGAGACGGAGTCTCGCT
CTGTCGCCCAGGTTGGAGTGAAGCGGCTAGATCTCAGCTCACTGCAACCTCTGCCTCCCAGGTTTA
AGCAATTCTCCTGTCTCAGCCTCCAGAGTAGCTGGGACTACAGGCGCATGCCACCATGCCCTACTA
ATTTTTTGTATTTTTAGGAGAGACAGGCCTTCACCATGTTGGTCAAGCTGGTCTCGAACTCCTGACC
TCAGGTGACCCACCGGCTTCAGCCTCCCAAAGTGCTGGGATTACAGGCATGAGCCACCGCGCCCA
GCCTCATATCTATCTTTATCACTCCATTTCAGATCTTCTTCCATATATGGCTCTGTGTGTCTCCTGTC
CTTCCCTGTCTCCTCACTGCTTTTCAGCTGGTAGACCCCTGTGGGGACAACAGATCAGAGCTTGGT
CACCAATATGGACATCTAGGTCTGAGCAGGGCCCACTCCCCGGGGGCGCATCAGCTCCATCCCGG
CACCCTTTACACTGGCCTTCTCTTCACAAAGGACCACAGGTCATCCTCAAGCCTTCCTCCCAGGCT
ATCCTTGTCCCTGAATACTAATGTCTAAAGGTCAGCCCAGCTACCAGCAGTGTGCATGTGATGTGT
CCCATCTCCCCTTCGGATTGGAGGAAGAAGCTGTGTCCCTCCCATCAGACAGACGGTCTCCTTAAA
GGTATTCTCCTGGTCTCCAGCTTGGGCTCTGCTGGAAAGAAGAGGAAGTATTTAGCAAGGGTGAAG
ATGGGTTCTTACTTCCCTGAGGCAACCAGAGATAAGAAAAGACCAGAATATGAATATCCAGCATTCC
ACAAAGAATCCTACAGGCAGGGATATTGCCCAATCACCAGTGCCTCGCATCCCAGTTCTATCCAAG
ATCCAAGCTTGATATCCTCCTGAAAGACTTCCTGAATCAGGTCACCAACATGGACATCTGAACTTCC
AGAATCAGGTCACCGTCTTTCTTCTCATCTCTGGATGTATTTGGAGCTCATTTGTCTGACGGTTTTTG
AATGCTATCTTTTAAAAATAAACTTTTACAATTTGGGTTTAATAATTCTAGATTTATAGAAAAGTTGAA
AAGAAAGTACAGAAAGTTCCCATATATCCCTTATCCAGTTCTCTTAATGTTAACCTCCTACATCATCA
TGGAACATTTGCCAAAATGAAGATGTCAACACTGGTGCTTTGCTGTGAACTAAACTCCAGACTTTAT
TCGGATTTCATGAATTTTTCTCCTAAGGTCCCTTTTCCGTTCCGGCATTCCACCCAGGATATCACATT
GCATTTGGTGTTTGTGTCTCCTTGGTCTCCTCTGGTTCTTGAGAGTTTCTCAGTCTCTCCTTGTTTTT
CGTGACTGAAGTTTCAAGGAGTACTGGTCAGGTATTCCATAGAATGTCCTACTGTTAGCTTTCAG

C

Fibrosis stage	Sample Number	Samples with TILAM
MASL	51	2 (3.9%)
MASH F0-F1	34	3 (8.8%)
MASH F2	53	3 (5.7%)
MASH F3	54	7 (13%)
MASH F4	14	4 (28.6%)

D

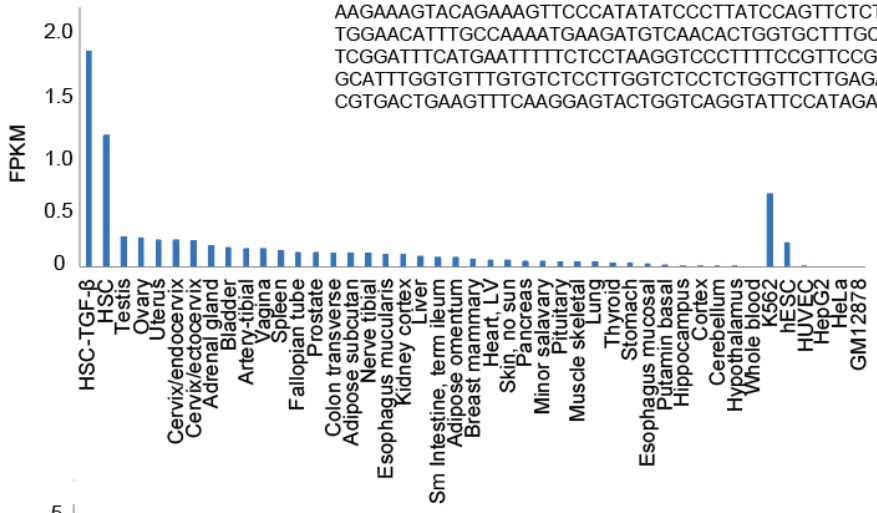

E

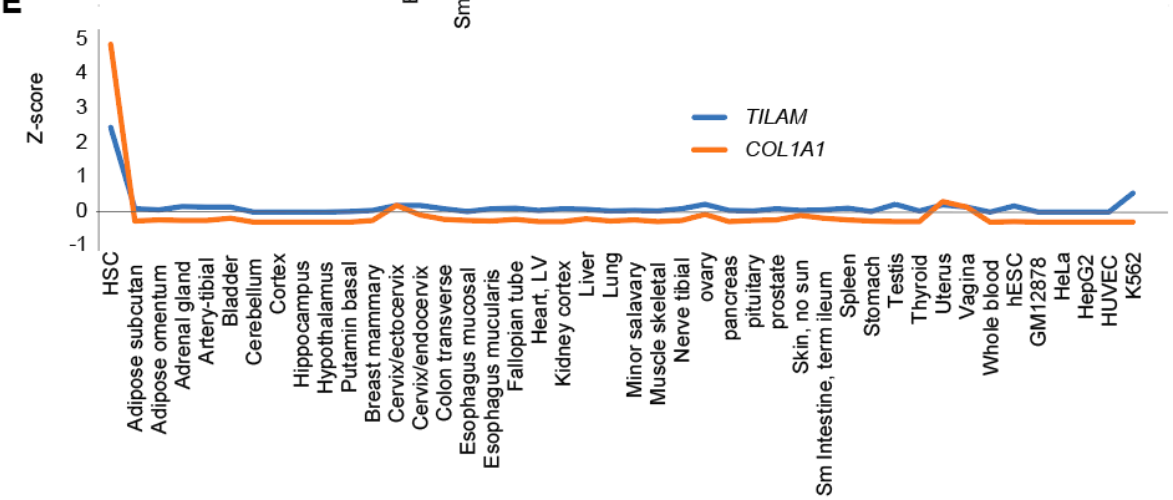

Supplemental Figure 1. Accessibility between *COL1A1* and *TILAM*, *TILAM* sequence cloned from human HSCs, and expression across tissues and cell types. (A) Formaldehyde assisted isolation of regulatory elements (FAIRE)(21) was performed followed by genomic qPCR to quantify relative accessibility (y-axis) of the *COL1A1* promoter, the *TILAM* promoter, and the region between both promoters (central region). Error bars represent mean ± SEM. (B) Sequence of the isoform of *TILAM* amplified from primary human HSCs. **(**D) *TILAM* gene expression (FPKM) was quantified across tissues and cell lines using previously published datasets(8). (D) *TILAM* and *COL1A1* expression (z-score) was analyzed across tissues and cell types (GTEx(22), GSE26284, and GSE41009)(8).

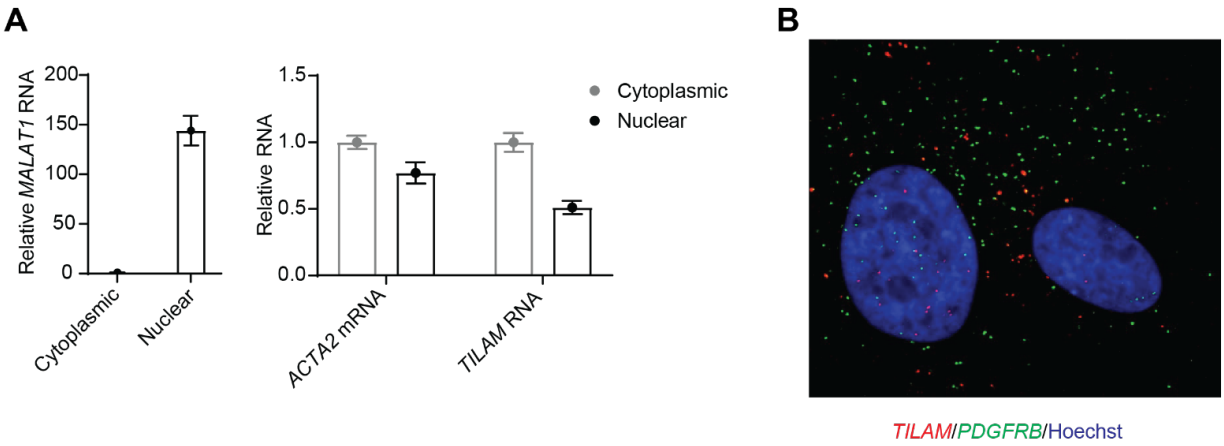
A
Relative MALAT1 RNA
200
150
100
50
0
Cytoplasmic
Nuclear
Relative RNA
1.5
1.0
0.5
0.0
Cytoplasmic
Nuclear
ACTA2 mRNA
TILAM RNA
B
TILAM/PDGFRB/Hoechst

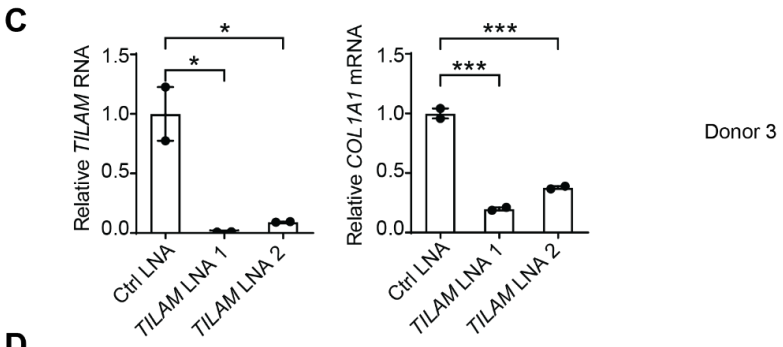
C
Relative TILAM RNA
Relative COL1A1 mRNA
Ctrl LNA
TILAM LNA 1
TILAM LNA 2
Donor 3

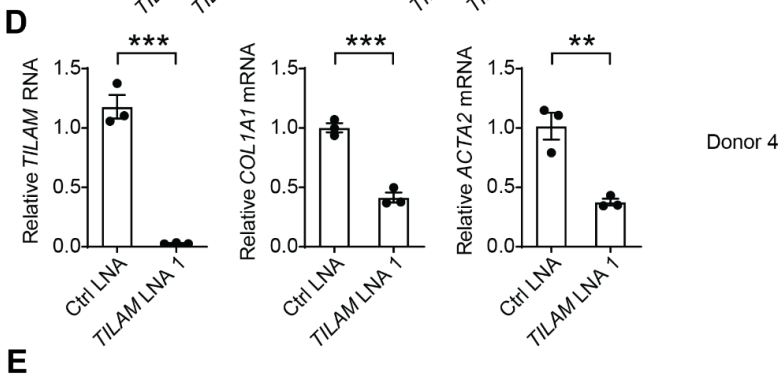
D
Relative TILAM RNA
Relative COL1A1 mRNA
Relative ACTA2 mRNA
Ctrl LNA
TILAM LNA 1
Donor 4

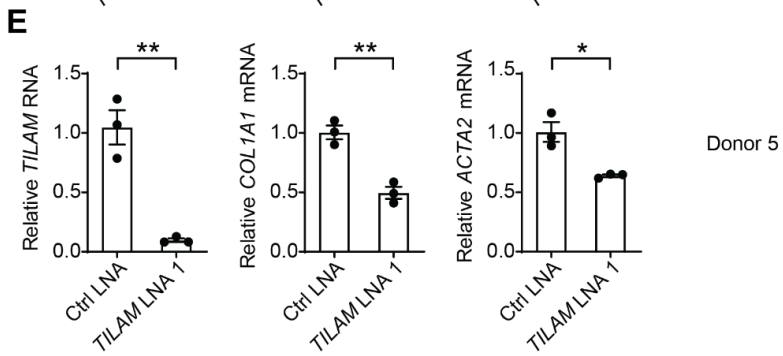
E
Relative TILAM RNA
Relative COL1A1 mRNA
Relative ACTA2 mRNA
Ctrl LNA
TILAM LNA 1
Donor 5

Supplemental Figure 2. Subcellular localization of *TILAM,* and depletion of *TILAM* in multiple primary human HSC lines. (A) Nuclear and cytoplasmic fractions from primary human HSCs were separated, and *MALAT1* transcripts were quantified by qRT-PCR (left) to assess efficiency of fractionation, as *MALAT1* is retained in the nucleus. The distribution of *ACTA2* and *TILAM* RNA transcripts were quantified in the nuclear and cytoplasmic fractions by qRT-PCR (right). Error bars represent mean ± SEM. (B) Single molecule RNA FISH (smFISH) was performed using probes that recognize *TILAM* (red) and *PDGFRB* (green). Nuclei are stained with Hoechst (blue). (C) Primary human HSCs from donor 3 were transfected with LNAs targeting *TILAM* (LNA 1 and LNA 2) and a control LNA before *TILAM* and *COL1A1* were quantified by qRT-PCR. * indicates $p<0.05$ and *** indicates $p<0.001$ (one-way ANOVA with Dunnett's multiple comparisons test). *GAPDH* was used as an endogenous control. (D-E) Primary human HSCs from two additional donors were transfected with *TILAM* LNA 1 and control LNA before *TILAM*, *ACTA2*, and *COL1A1* were quantified by qRT-PCR. * indicates $p<0.05$, ** indicates $p<0.01$, *** indicates $p<0.001$ (2-tailed unpaired *t* test). *GAPDH* was used as an endogenous control.

A

Disruption of human *TILAM* locus

B

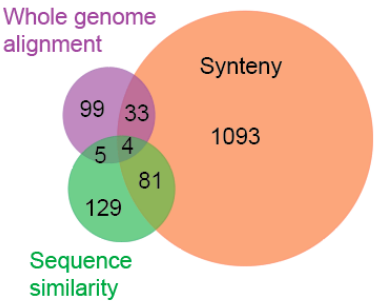

C

D

AAATTTTCCCAAATGTTTCCCCCCCCACGAGGGAGGGAGAAGACCCGTCTGGACTCTACGGTGTGGAACAGAAGC
AGAGGCAGCCTAGGTATAAATGTAGCAGACCTTCCAGCCGTTCACTCTGTCCATCTACAGAAGCAGCAGATGTGGG
AGAGACGGCATGAAAGACAAGACCACCATATCATTCCAGCCCGAATCTGGGAGCCCCGGACAGTCCCAGACAGCA
GCTCCAGGCCCTCAGCTGGGCCCTGTGACCAGAGGGGGAAGGGAGCATGGTGGGCAGGGAGGAACTGCCACCT
GGAAGGGCTTGATGGGAACCAGCTGGCTGGGGTGGGGCCTCGGGTGTGTGGGTTGCAGGGAGGGCGGGGCAA
GACAGGGCAGCAGGCCACAGTGGGCGGGCAACTGACAGCGCTGGGCTGGGAGTGGCTGCTGGAGGCCCCCAC
CTTCCCGAAGGCTGGAGTCCAGATGCCTCTACAGCCGGCCAGGCTCTTCCAACCCGCTGACCTCATTCCCAGCTC
CCGCCCGTGCAGCCCCCCTCAACTGCCTGCCACGTAGACTAGAGCCTCAGCAGGACTCCGTAGGGGTGGCTGCA
AGAGGGCCCAGGCACCCTTAGCCTAGAAACCTGCTCAGAGAGACAGAGCTAGGGAAGGTAGCTGTGACCACTTG
GTGCCTCAGTTTCCCTTCCCCAAATATGAGTCCCAGTGAATGGAGAGGAGCTAAGTGTGAAGCAGGTTAGAGTTGC
CAAACAAGAGTCAAGGTGGGGGTGAGAGGGAGGTCCCTAGAGGTCATCCCAGCCATCCCTCAGTTTCTTAAGTTT
GGGGAGTATTGCTCTCAAGAAGAGGCAGAGGCACCGGGGGGTGGGGGTGGGATGTGGGGTGGGGTGTGAGTGGG
GTGGGGGATGGGGTGTGAGGGGCGGGGGAAGGCAGGTTCCCTCCTTTGTCAAACTATTCAAATGAATGGAAGTTC
CCAGAA

E

CCGCCCCTCACACCCCATCCCCCACCCCACTCACACCCCACCCCACATCCCACCCCCACCCCC

F

```
TILAM   269  GCTGCAGCCCAGATGCCTTCGCAGCCATGGCCTGGCCCATCCAACCCGCTGACCTCATTC  328
             ||||  ||  ||||||||||   |||||  ||||  |||  |  ||||||||||||||||||||
Tilam   354  GCTGGAGTCCAGATGCCTCTACAGCC--GGCCAGGCTCTTCCAACCCGCTGACCTCATTC  411

TILAM   329  CCAGCTCCCCTCTCTTGCAAGCTCCCC-C-CTTGCCTGCCACGTAGACTGGAGGCTTAGC  386
             |||||||||   |  |  ||||  ||  ||||  |   ||||||||||||||||  |||  ||  |||
Tilam   412  CCAGCTCCCGCC-CGTGCA-GCCCCCCTCAACTGCCTGCCACGTAGACTAGAGCCTCAGC  469
```

Supplemental Figure 3. Disruption of human *TILAM* for human liver organoid differentiation and sequence of murine *Tilam* and alignment with human *TILAM*. (A) Homology directed repair (HDR) was performed to insert a cDNA encoding GFP and polyadenylation (polyA) signal into *TILAM* to disrupt expression of the lncRNA (orange line indicating termination of transcription). HDR was performed using a plasmid containing a puromycin expression cassette. Puro-resistant hESCs were screened to identify clones where both *TILAM* genes were disrupted. (B) Venn diagram showing murine lncRNAs with human orthologs as determined by synteny, whole genome alignment, and sequence similarity. (B) Schematic of *Tilam* in relation to *Col1a1* in the mouse genome. (C) Sequence of *Tilam* cloned from murine HSCs. (D) Repetitive sequence in 63 nt gap between two transcripts in the *Tilam* locus assembled with RNA-seq data from murine HSCs (Figure 3F*)*. (E) Sequence conservation between human (top) and murine *(bottom) TILAM* at indicated nucleotide positions. Nucleotide positions are based on cloned sequences (Supplemental Figure 1B and Supplemental Figure 3D).

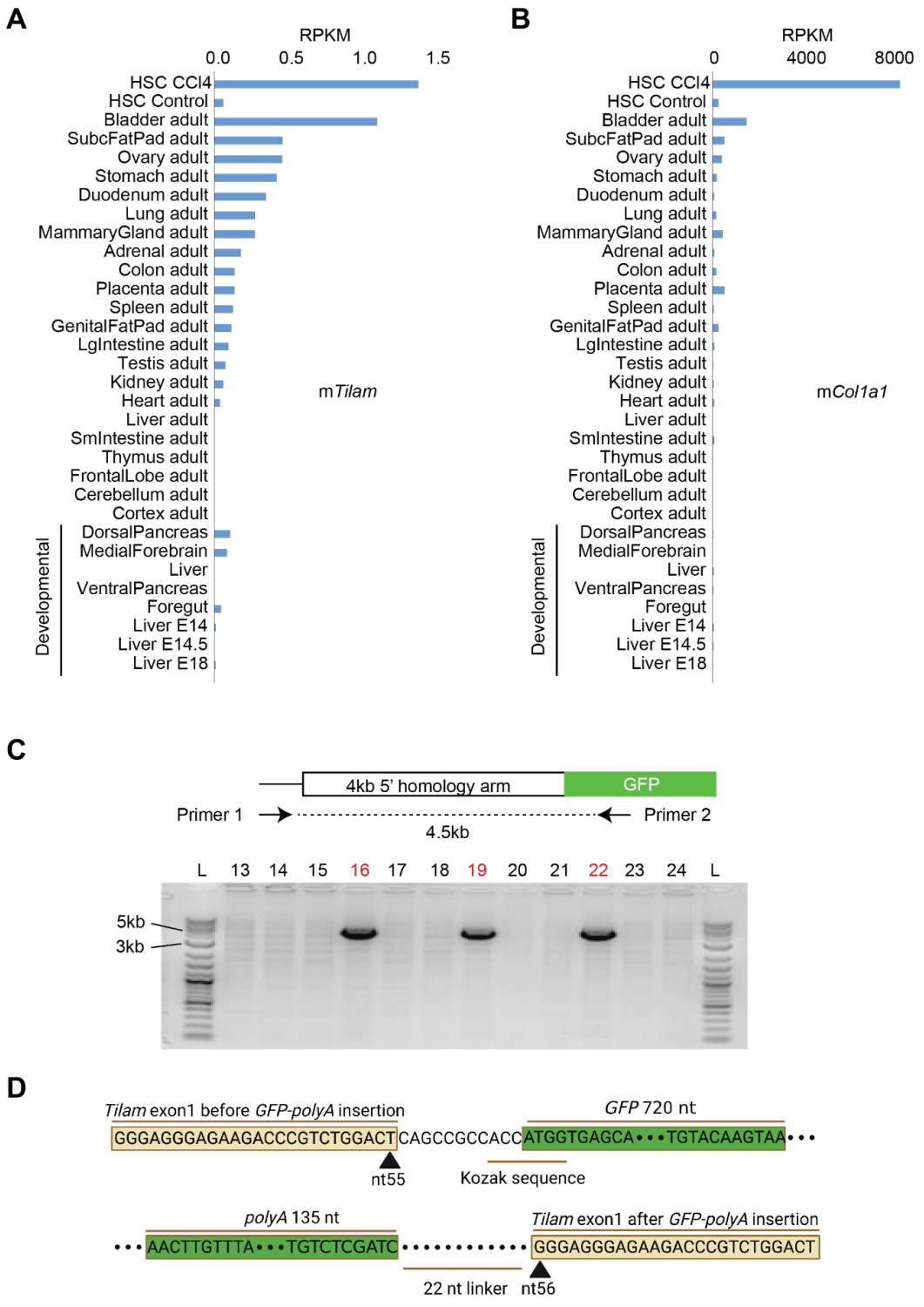
A
RPKM
0.0
0.5
1.0
1.5
HSC CCl4
HSC Control
Bladder adult
SubcFatPad adult
Ovary adult
Stomach adult
Duodenum adult
Lung adult
MammaryGland adult
Adrenal adult
Colon adult
Placenta adult
Spleen adult
GenitalFatPad adult
LgIntestine adult
Testis adult
Kidney adult
Heart adult
Liver adult
SmIntestine adult
Thymus adult
FrontalLobe adult
Cerebellum adult
Cortex adult
DorsalPancreas
MedialForebrain
Liver
VentralPancreas
Foregut
Liver E14
Liver E14.5
Liver E18
Developmental
mTilam
B
RPKM
0
4000
8000
HSC CCl4
HSC Control
Bladder adult
SubcFatPad adult
Ovary adult
Stomach adult
Duodenum adult
Lung adult
MammaryGland adult
Adrenal adult
Colon adult
Placenta adult
Spleen adult
GenitalFatPad adult
LgIntestine adult
Testis adult
Kidney adult
Heart adult
Liver adult
SmIntestine adult
Thymus adult
FrontalLobe adult
Cerebellum adult
Cortex adult
DorsalPancreas
MedialForebrain
Liver
VentralPancreas
Foregut
Liver E14
Liver E14.5
Liver E18
Developmental
mCol1a1
C
4kb 5' homology arm
GFP
Primer 1
Primer 2
4.5kb
L 13 14 15 16 17 18 19 20 21 22 23 24 L
5kb
3kb
D
Tilam exon1 before GFP-polyA insertion
GFP 720 nt
GGGAGGGAGAAGACCCGTCTGGACT CAGCCGCCACC ATGGTGAGCA•••TGTACAAGTAA•••
nt55
Kozak sequence
polyA 135 nt
Tilam exon1 after GFP-polyA insertion
•••AACTTGTTTA•••TGTCTCGATC••••••••••••
GGGAGGGAGAAGACCCGTCTGGACT
22 nt linker
nt56

Supplemental Figure 4. *Tilam* expression and insertion of *GFP* and a polyadenylation (polyA) signal to disrupt the *Tilam* gene. (A-B) Murine *Tilam* and *Col1a1* expression patterns across adult and developmental tissues (GSE36025 and GSE36114) compared to murine HSCs isolated from mice with or without CCl_4 treatment in this study. (C) Genomic PCR performed on pups born after zygote injections for genome editing to identify founders. The upstream primer (Primer 1) annealed to a region located outside the 4 kb homology arm used for homologous recombination while the downstream primer (Primer 2) annealed to a region within the *GFP* sequence. Products were visualized on an agarose gel. Mice 16, 19, and 22 (red) showed evidence of the correct insertion. These mice were crossed to wild-type C57BL/6 mice to confirm germline transmission and back crossed for six generations to wild-type C57BL/6 mice before intercrossing mice from the same founders. DNA ladder (L) is on the left and right, with 3kb and 5kb markers indicated on the left. (D) Sequencing of genomic DNA was performed in $Tilam^{gfp/gfp}$ mice, showing insertion of *GFP*-polyA sequence at nt 55 of exon 1. The complete sequence was truncated to show sites of insertion.

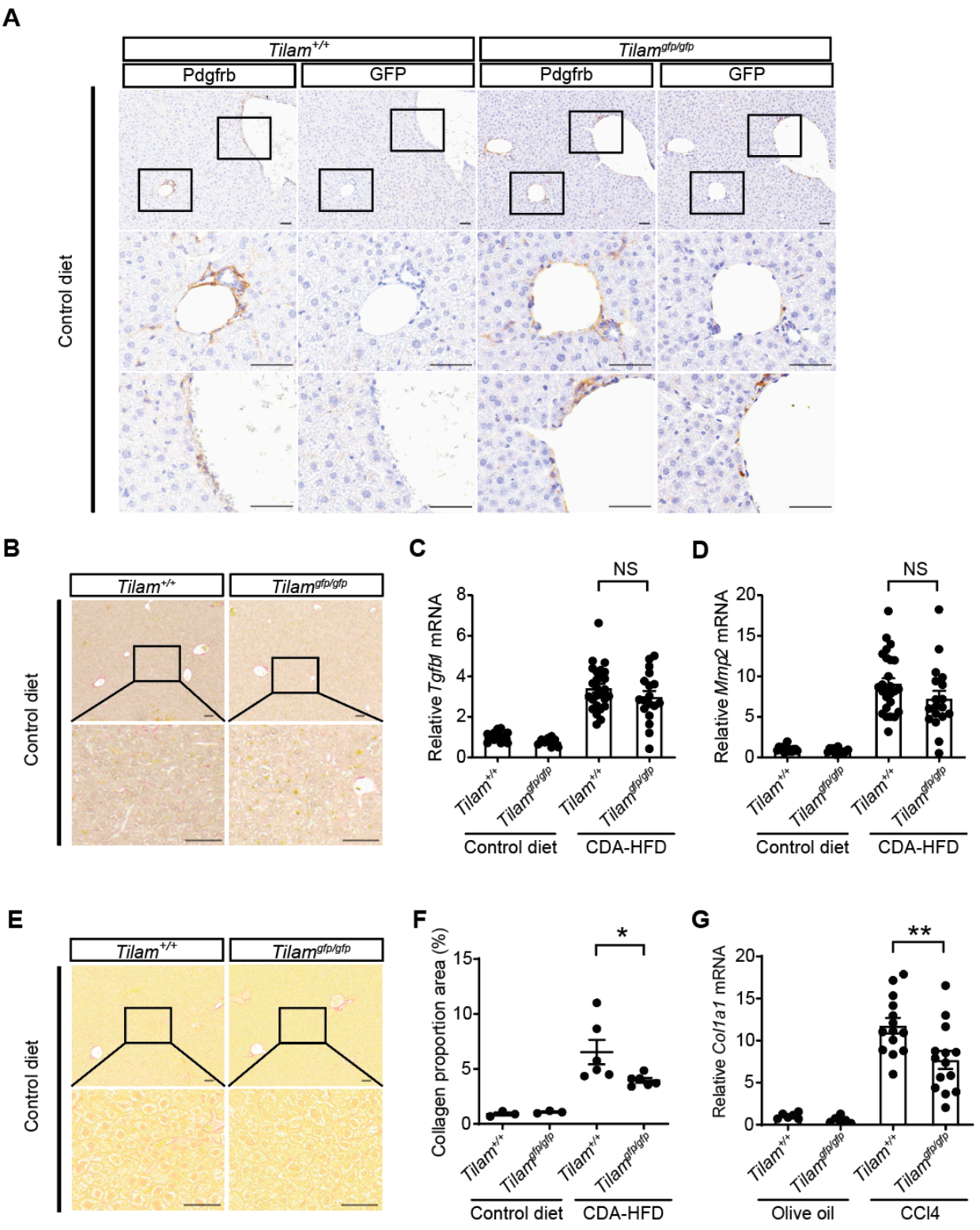
A
Tilam+/+
Tilamgfp/gfp
Pdgfrb
GFP
Pdgfrb
GFP
Control diet
B
Tilam+/+
Tilamgfp/gfp
Control diet
C
NS
Relative Tgfb1 mRNA
Tilam+/+
Tilamgfp/gfp
Tilam+/+
Tilamgfp/gfp
Control diet
CDA-HFD
D
NS
Relative Mmp2 mRNA
Tilam+/+
Tilamgfp/gfp
Tilam+/+
Tilamgfp/gfp
Control diet
CDA-HFD
E
Tilam+/+
Tilamgfp/gfp
Control diet
F
*
Collagen proportion area (%)
Tilam+/+
Tilamgfp/gfp
Tilam+/+
Tilamgfp/gfp
Control diet
CDA-HFD
G
**
Relative Col1a1 mRNA
Tilam+/+
Tilamgfp/gfp
Tilam+/+
Tilamgfp/gfp
Olive oil
CCl4

Supplemental Figure 5. IHC for GFP and Sirius red in control conditions and *additional* analysis of CDA-HFD and CCl_4 experiments. (A) IHC of Pdgfrb and GFP in *Tilam*$^{gfp/gfp}$ and *Tilam*$^{+/+}$ and livers with normal diet. Pdgfrb is limited to the periportal area and vessels in normal diet and a small number of GFP positive cells are detected in similar regions of *Tilam*$^{gfp/gfp}$ mice with control diet. Scale bar: 50 μm. (B) Representative images of Sirius red staining in *Tilam*$^{gfp/gfp}$ and *Tilam*$^{+/+}$ female mice receiving control diet for CDA-HFD in experiment Figure 5C. Scale bar = 50 μm. (C) *Tgfb1* expression was quantified by qRT-PCR in female mice receiving CDA-HFD or control diet (n=13, 12, 26, 18). Error bars represent mean ± SEM. ns indicates $p>0.05$ (2-tailed unpaired *t* test). *Gapdh* was used as an endogenous control. (D) *Mmp2* expression was quantified by qRT-PCR in female mice receiving CDA-HFD or control diet (n=13, 12, 26, 18). ns indicates $p>0.05$ (2-tailed unpaired *t* test). *Gapdh* was used as an endogenous control. (E) Representative images of Sirius red staining in *Tilam*$^{gfp/gfp}$ and *Tilam*$^{+/+}$ male mice receiving control diet for CDA-HFD in experiment Figure 5H. Scale bar = 50 μm. (F) Collagen proportionate area (CPA) was calculated for the indicated conditions in male mice receiving CDA-HFD (Figure 5G-H). Samples closest to the mean for each condition in Figure 5G were selected for analysis (n=3, 3, 6, 6). * indicates $p<0.05$ (2-tailed unpaired *t* test). (G) *Col1a1* expression was quantified by qRT-PCR in male mice after 4 weeks of CCl_4 treatment (n=6, 6, 14, 14). ** indicates $p<0.01$ (2-tailed unpaired *t* test). Error bars represent mean ± SEM. *Gapdh* was used as an endogenous control.

scTILAM-apt

TGCGGCCGCCGACCAGAATCATGCAAGTGCGTAAGATAGTCGCGGGTCGGCGGCCGCATCTGCTG
GGAGATCCGTAGAAAATGCGGCCGCCGACCAGAATCATGCAAGTGCGTAAGATAGTCGCGGGTCG
GCGGCCGCATCTGCTGGGAGATCCGTAGAAAATGCGGCCGCCGACCAGAATCATGCAAGTGCGTAA
GATAGTCGCGGGTCGGCGGCCGCATCTGCTGGGAGATCCGTAGAAAATGCGGCCGCCGACCAGAA
TCATGCAAGTGCGTAAGATAGTCGCGGGTCGGCGGCCGCATCTGCTGGGAGATCTGATATCATCGA
TGAATTCGAGCTCGGTAGAGCTCGGTACGTAATTAGCACCCTGCTTACTAAGGATTGAACCTCCTTC
CGATGTCGCACCGAGCTAGTAGTGATCGTATCTGTGATATGGGGAAAGAAAGTGGTATCGTCTCTGT
GCCTTAGAGACCGATAGGAACAGACCCCCCAATTTCGCGCGGACGCCCCTACGCCCAACCTGAGAT
GCTTGTCCTTAGCCGTCCTGTGGCGAGAGCAGTCTCATGGTTACCTTGTCCACTTCAGGGGAGGCG
CAATCAGTAGGGCGTAATCCCAGCTAATCCCTCTGCTGAGTCCTTCACATGAAGAACCTCCAGAAAT
TGAGTGATCTCAGGACATAAGTTGCCAGAAAGCCTTTGCCTGCGAACTACGGGCTTACAAAACATTA
GCCAAAAGCTTCAACAAATGATATCTGCCCACCCGAGTGAAGACGGGCCGATTGCGAGCGGATCTT
GTTCGATAGTAATATCTGTTTGTTAAGGTACACGGCAAATCATGGCCAGCGCGCCAGATCCACACTC
CACCCTAGAACACACCGACGGAGGTGTCGTGCCGCGTAGGGGTTCTGTGTGGAATCTTGCTTTAAC
CGCGCTATATTAATGTGATATTCAATTTCAGACGCCTCGTTGCTCATAACGTTCACAATACATTTCCCC
ATTCGAATTTACATTCTACACAGGGAAAAAATCACGGTCCCTACACCTAGCGACTTGTGTCTGTGCGT
CCGGGTGGACAATATTCGTCTTACCCATCGGGCTCACCGTCCTCCCCGTCGCAGTATACCCTCTTCA
GGACTCGTAGGGGGGGCTATGTGGCCCAGCGGCCATGAATGCACTAATATCAGCGGACTCTGCGAT
AGTGGGCTGACCGGCGAGTGGGACTAGGCTTGTCCGCCGCGGAACGCGTTTCAGGCAGACCGTGT
CCAGTGCGAAATCATGGGGCATTGTTTACGTAAATAGGTCGACATGTTCAGGGCATAGTGAATTTAT
CATATGCTGTACGCTTGGTCCGCCTTGAGGAGTGCCGTGCAGTCTCGTGATTAGAGTACACGTAGTG
GTTCCGCGCGAACGAAAGGTGAGACCCACCCCCCGCGCTGGGTGGGCTAGGTAACGCCTATTGTTA
ACATCTGAATTCGGGACCACATATAGTAAATGAAGTTTAGGTTCTCATCTCCTAACTTGAGCCATCGA
TGGGAACGTTCGAATTTCCTCTAACGGTAGTCAGGCAGTGAACTCTGATTCCTAGGCTTGGCCAGCC
CCGCAGAACATGTCTCGTTGGTCGGTCGCATCTGAAGGACGTGCGGGCGTCATGTCTTTGCTCTATT
GTTCACAAGGGAGGAACTCTAGCTCATAGCTGCACTATGCCCACAGCTTTGTCTCCTATGATTACGG
CTTGGGTCGGACACAAGCACTTCGAACATTAACCTCGGGAGCATTACTCTAATGCGGCATTTAAAAC
AAACGCTGGACGGCACACAGTTGGAATACTAGTCAGAACTATCTTGTATTGGGCAGTGAACACCCGC
TGCTCGTAACTTCACGAATCTTTCTAGTGTCCGTGCAGTAAAAAGACATCGCTTGGCACCCTCTTCCA
ATCATGGATCTATAGTAAATCCTTGCGGCTGGTCTATATGAAATATGGCCGAGCTGGTCACCACGTC
CGTTAAGTCCGAATTGCCCGTGCTCTTGCTAACCCAGAGTACCGTCCTGCACCCGCTACTCTAAATC
TTGTCGTACTGGATTGTATACTACATCATCGATTTCGGCTCGCGGACTGGTATTCATACACGCTCGC
GCCCTTTCAAACGAAGTCCTATACTTTATACAATCGGGACATCCCCTACCGAATACGTCTACCGCAAT
TAAGCCCCATGACTTCGTCTCCTAGGGAACGTTATTAAGCGACTGTGGCGCTGATTACCGCCATAGT
TTTTTCGATCTCTCCACGCACATGATCTCATAACTGCACACCGTGTCCCTCCGTCATGTCATCTAGAC
CGATGGTGAACCACTAAATGCCGTTGTAGTTTGGGGGTATAGTCAATCAGGAAAGGATAGGTGCAGA
TCATCTCTTTATGTTGTGCGTGTGATGCACGGCGTCAACTGCTACCCCCGTAGCGTTCTGACTCTCG
CTTGGTGATTGCTACGCTGACATGGTTGCATTGGGCTGGGACACTTGACAAATCCCAGTGCCGGAG
CCGACTGTCTTATGTACGTTTGCCAATTAACAGCGTGAATCTTATCCACTCGAACCAAAATTACATTT
GTCACCGAGTTGCCGCAGCATGACCAGAGGACCTGGGTCCGGTAGCAGATGACGACAGTCCGTCA
GATTAGTAACGTATTCACCC

Supplemental Figure 6. Sequence of scrambled *TILAM* with aptamer (*scTILAM-apt*). The nucleotide sequence of *TILAM was scrambled* and fused to the 4 x S1m aptamer sequence(11,23). The aptamer sequence is shown in blue, and the scrambled (*sc) TILAM* sequence is shown in black. *TILAM*-apt contains the same sequence as in Supplemental Figure 1B and is fused to the same aptamer sequence on the 5' end (blue) of *scTILAM*.

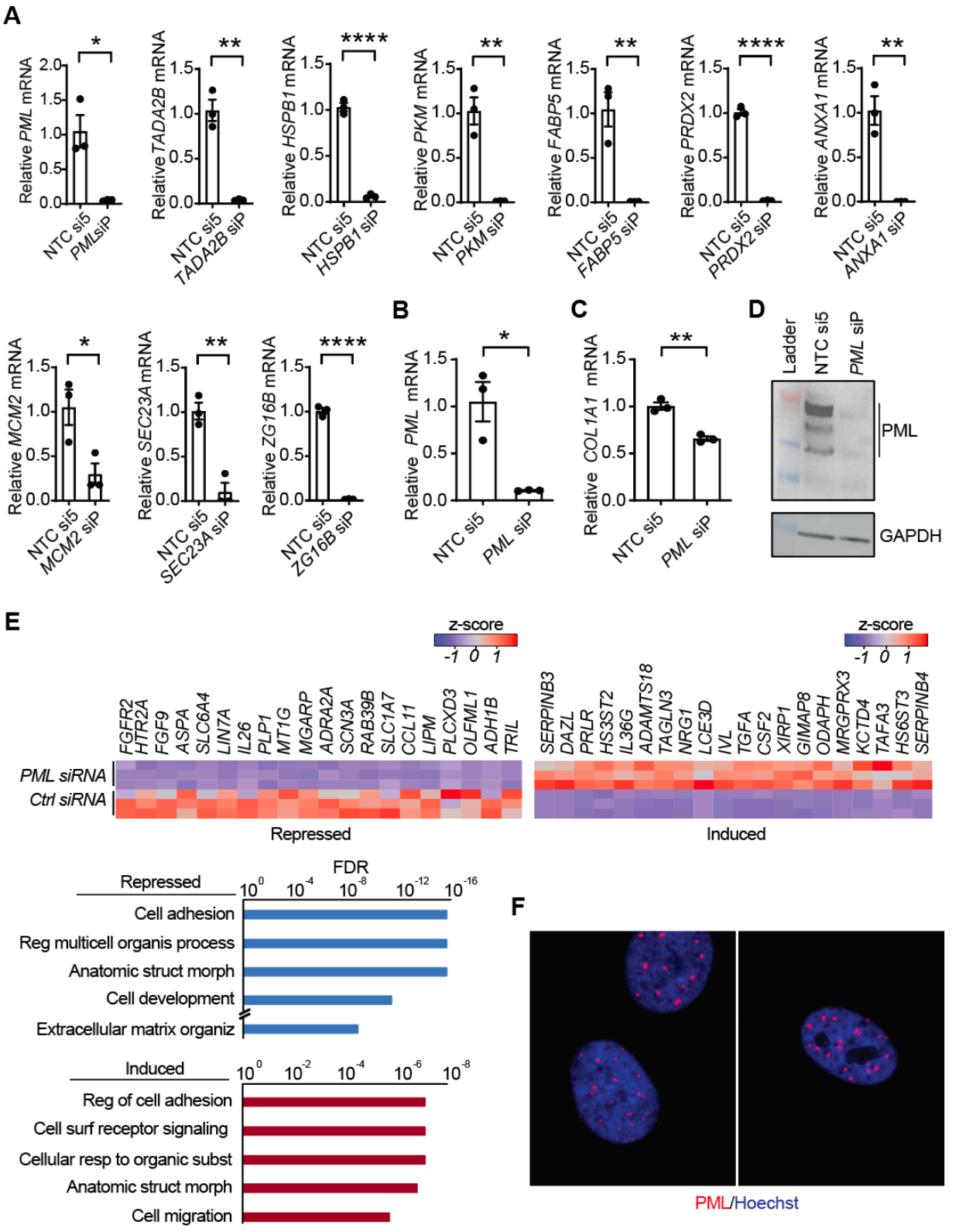
A
Relative PML mRNA
NTC si5
PMLsiP
Relative TADA2B mRNA
TADA2B siP
Relative HSPB1 mRNA
HSPB1 siP
Relative PKM mRNA
PKM siP
Relative FABP5 mRNA
FABP5 siP
Relative PRDX2 mRNA
PRDX2 siP
Relative ANXA1 mRNA
ANXA1 siP
Relative MCM2 mRNA
MCM2 siP
Relative SEC23A mRNA
SEC23A siP
Relative ZG16B mRNA
ZG16B siP
B
Relative PML mRNA
PML siP
C
Relative COL1A1 mRNA
D
Ladder
PML
GAPDH
E
z-score
-1 0 1
FGFR2 HTR2A FGF9 ASPA SLC6A4 LIN7A IL26 PLP1 MT1G MGARP ADRA2A SCN3A RAB39B SLC1A7 CCL11 LIPM PLCXD3 OLFML1 ADH1B TRIL
SERPINB3 DAZL PRLR HS3ST2 IL36G ADAMTS18 TAGLN3 NRG1 LCE3D IVL TGFA CSF2 XIRP1 GIMAP8 ODAPH MRGPRX3 KCTD4 TAFA3 HS6ST3 SERPINB4
PML siRNA
Ctrl siRNA
Repressed
Induced
FDR
Repressed
Cell adhesion
Reg multicell organis process
Anatomic struct morph
Cell development
Extracellular matrix organiz
Induced
Reg of cell adhesion
Cell surf receptor signaling
Cellular resp to organic subst
Anatomic struct morph
Cell migration
F
PML/Hoechst

Supplemental Figure 7. Depletion of products identified by MS, *PML* depletion leads to reduced *COL1A1* expression in primary HSC lines from an additional donor, and depletion of PML leads to broader effects on ECM production as quantified by RNA-seq. (A) mRNAs encoding the proteins most enriched with *TILAM-apt* precipitation (Figure 6B and 6C) were depleted in primary human HSCs using pooled siRNAs. Depletion of each target was quantified by qRT-PCR compared to control siRNA (NTC 5). * indicates $p<0.05$, ** indicates $p<.0.1$, *** indicates $p<0.001$, **** indicates $p<0.001$ (2-tailed unpaired *t* test). Error bars represent mean ± SEM. *GAPDH* was used as an endogenous control. (B-C) *PML* was depleted in primary human HSCs from donor 5 using pooled siRNAs against *PML* mRNA and a control siRNA (NTC 5). *PML* and *COL1A1* levels were quantified by qRT-PCR. * indicates $p<0.05$, ** indicates $p<0.01$ (2-tailed unpaired *t* test). Error bars represent mean ± SEM. *GAPDH* was used as an endogenous control. (D) PML protein was quantified by Western blot following depletion with *PML* siP compared to non-targeting control (NTC si5). The molecular weight ladder is included (left). GAPDH was evaluated as a loading control. (E) Heatmaps show the relative expression of the top 20 genes repressed (left) and induced (right) with depletion of *PML*. GO analysis was performed on genes repressed (blue) and induced (red) with depletion of *PML*. False discovery rate (FDR) is indicated on the x-axis. (F) IF was performed in primary human HSCs using an antibody against PML (red). Nuclei are stained with Hoechst (blue). Three nuclei probed for PML are shown.

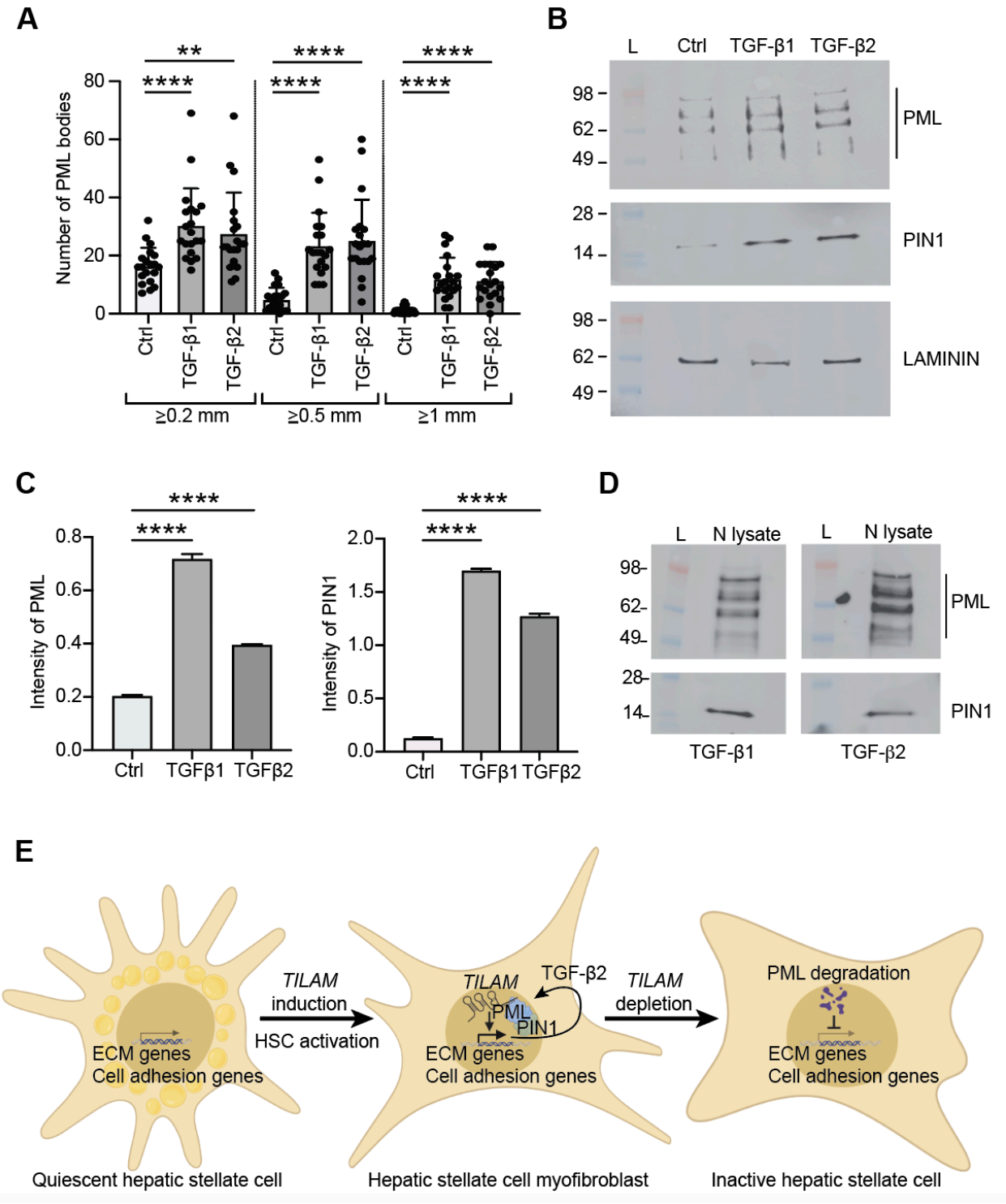
A
Number of PML bodies
Ctrl
TGF-β1
TGF-β2
≥0.2 mm
≥0.5 mm
≥1 mm
B
L
Ctrl
TGF-β1
TGF-β2
PML
PIN1
LAMININ
C
Intensity of PML
Intensity of PIN1
Ctrl
TGFβ1
TGFβ2
D
L
N lysate
PML
PIN1
TGF-β1
TGF-β2
E
TILAM
induction
HSC activation
TILAM
TGF-β2
PML
PIN1
TILAM
depletion
PML degradation
ECM genes
Cell adhesion genes
Quiescent hepatic stellate cell
Hepatic stellate cell myofibroblast
Inactive hepatic stellate cell

Supplemental Figure 8. Size of nuclear bodies and nuclear localization in response to TGF-β signaling and schematic showing how *TILAM* promotes liver fibrosis. (A) Sizes of PML nuclear bodies were quantified following treatment with TGF-β1 (10 ng/ml), TGF-β2 (10 ng/ml), or control conditions for 6 hr at indicated thresholds. Each dot represents a single nucleus. ** indicates $p<0.01$ and **** indicates $p<0.0001$ (one-way ANOVA with Dunnett's multiple comparison). Error bars represent mean ± SEM. Results are representative of two independent experiments. (B) Expression of PML and PIN1 was quantified by Western blot in HSC nuclear lysates after treatment with TGF-β1 (10 ng/ml), TGF-β2 (10 ng/ml), or control conditions for 6 hr. LAMININ was quantified as a loading control. Molecular weight markers for the ladder (L) are indicated on the left (in kilodaltons). Data are representative of two independent experiments. (C) Expression of PML and PIN1 from (B) were normalized to LAMININ expression for quantification. **** indicates $p<0.0001$ (one-way ANOVA with Dunnett's multiple comparison). Error bars represent mean ± SEM. Results are representative of two independent experiments. Data are representative of three independent experiments. (D) PML (top) and PIN1 protein levels (bottom) were quantified in nuclear lysates (N lysates) by Western blot prior to co-immunoprecipitation experiments (Figure 7G). Molecular weight markers for the ladder (L) are indicated on the left (in kilodaltons). HSCs were treated with TGF-β1 (10 ng/ml) or TGF-β2 (10 ng/ml) for 6 hr prior to harvest as indicated. (E) MODEL: *TILAM* is not expressed in quiescent HSCs, and expression of collagen and other extracellular matrix (ECM) genes is low (left). With transdifferentiation to HSC myofibroblasts, *TILAM* expression is induced, and *TILAM* interacts with PML protein to promote expression of genes involved in ECM production and cellular adhesion (center). This includes regulation of TGF-β2, which promotes expression of *TILAM* and nuclear localization of PML and PIN1 to further promote gene expression. When *TILAM* is depleted in HSC myofibroblasts PML protein levels fall, and ECM and adhesion gene expression is repressed (right). All data shown were performed in HSC donor 2.

Supplemental Datasets

Supplemental Dataset 1. Nucleotide sequences

Supplemental Dataset 2. List of antibodies

Supplemental Dataset 3. Probes for single molecule fluorescent in situ hybridization.

Supplemental Dataset 4. RNA-seq analysis of *TILAM* and PML depletion

Supplemental Dataset 5. Genomic location of murine lncRNAs

Supplemental Dataset 6. Classification of murine lncRNAs

Supplemental Dataset 7. Expression of murine lncRNAs in HSCs in vivo

Supplemental Dataset 8. Conserved lncRNAs that are regulated by CCl_4 treatment

Supplemental Dataset 9. Mass spectrometry data

Note: all supplemental datasets are provided as Excel files

Supplemental References

1. Fujii T, Fuchs BC, Yamada S, Lauwers GY, Kulu Y, Goodwin JM, et al. Mouse model of carbon tetrachloride induced liver fibrosis: Histopathological changes and expression of CD133 and epidermal growth factor. BMC Gastroenterol. 2010;10:79.
2. Matsumoto M, Hada N, Sakamaki Y, Uno A, Shiga T, Tanaka C, et al. An improved mouse model that rapidly develops fibrosis in non-alcoholic steatohepatitis. International journal of experimental pathology. 2013;94:93–103.
3. Wei G, An P, Vaid KA, Nasser I, Huang P, Tan L, et al. Comparison of murine steatohepatitis models identifies a dietary intervention with robust fibrosis, ductular reaction, and rapid progression to cirrhosis and cancer. Am J Physiol-gastr L. 2020;318:G174–G188.
4. **Mederacke I**, **Hsu CC**, **Troeger JS**, Huebener P, Mu X, Dapito DH, et al. Fate tracing reveals hepatic stellate cells as dominant contributors to liver fibrosis independent of its aetiology. Nature Communications. 2013;4:1–11.
5. Mederacke I, Dapito DH, ograve SA, Uchinami H, Schwabe RF. High-yield and high-purity isolation of hepatic stellate cells from normal and fibrotic mouse livers. Nature Protocols. 2015;10:305–315.
6. Li W, Chen JY, Sun C, Sparks RP, Pantano L, Rahman R-U, et al. Nanchangmycin regulates FYN, PTK2, and MAPK1/3 to control the fibrotic activity of human hepatic stellate cells. Elife. 2022;11:e74513.
7. Kim B-M, Abdelfattah AM, Vasan R, Fuchs BC, Choi MY. Hepatic stellate cells secrete Ccl5 to induce hepatocyte steatosis. Sci. Rep. 2018;8:7499.
8. Zhou C, York SR, Chen JY, Pondick JV, Motola DL, Chung RT, et al. Long noncoding RNAs expressed in human hepatic stellate cells form networks with extracellular matrix proteins. Genome Medicine. 2016;1–20.
9. **Govaere O**, **Cockell S**, Tiniakos D, Queen R, Younes R, Vacca M, et al. Transcriptomic profiling across the nonalcoholic fatty liver disease spectrum reveals gene signatures for steatohepatitis and fibrosis. Sci. Transl. Med. 2020;12.
10. Liao Y, Smyth GK, Shi W. featureCounts: an efficient general purpose program for assigning sequence reads to genomic features. Bioinformatics. 2014;30:923–930.
11. Daneshvar K, Ardehali MB, Klein IA, Hsieh F-K, Kratkiewicz AJ, Mahpour A, et al. lncRNA DIGIT and BRD3 protein form phase-separated condensates to regulate endoderm differentiation. Nature Cell Biology. 2020;1–32.
12. **Ouchi R**, **Togo S**, Kimura M, Shinozawa T, Koido M, Koike H, et al. Modeling Steatohepatitis in Humans with Pluripotent Stem Cell-Derived Organoids. Cell Metabolism. 2019;30:374-384.e6.
13. Hess A, Gentile SD, Saad AB, Rahman R-U, Habboub T, Mullen AC. Human liver organoids model progressive inflammatory and fibrotic injury in non-alcoholic fatty liver disease. Biorxiv. 2022;2022.07.19.500693.
14. Daneshvar K, Pondick JV, Kim B-M, Zhou C, York SR, Macklin JA, et al. DIGIT Is a Conserved Long Noncoding RNA that Regulates GSC Expression to Control Definitive Endoderm Differentiation of Embryonic Stem Cells. Cell Reports [Internet]. 2016;17:353–365. Available from: http://apply.pewscholars.org/form.php
15. Liao Y, Wang J, Jaehnig EJ, Shi Z, Zhang B. WebGestalt 2019: gene set analysis toolkit

with revamped UIs and APIs. Nucleic Acids Res. 2019;47:W199–W205.
16. **Yang W**, **He H**, Wang T, Su N, Zhang F, Jiang K, et al. Single-Cell Transcriptomic Analysis Reveals a Hepatic Stellate Cell–Activation Roadmap and Myofibroblast Origin During Liver Fibrosis in Mice. Hepatology. 2021;74:2774–2790.
17. Kent WJ. BLAT—The BLAST-Like Alignment Tool. Genome Res. 2002;12:656–664.
18. Satija R, Farrell JA, Gennert D, Schier AF, Regev A. Spatial reconstruction of single-cell gene expression data. Nat. Biotechnol. 2015;33:495–502.
19. Ikenaga N, Peng Z-W, Vaid KA, Liu SB, Yoshida S, Sverdlov DY, et al. Selective targeting of lysyl oxidase-like 2 (LOXL2) suppresses hepatic fibrosis progression and accelerates its reversal. Gut. 2017;66:1697.
20. Sojoodi M, Erstad DJ, Barrett SC, Salloum S, Zhu S, Qian T, et al. Peroxidasin Deficiency Re-programs Macrophages Toward Pro-fibrolysis Function and Promotes Collagen Resolution in Liver. Cell Mol Gastroenterology Hepatology. 2022;13:1483–1509.
21. Giresi PG, Kim J, McDaniell RM, Iyer VR, Lieb JD. FAIRE (Formaldehyde-Assisted Isolation of Regulatory Elements) isolates active regulatory elements from human chromatin. Genome Res. 2007;17:877–885.
22. Consortium TGte, Ardlie KG, Deluca DS, Segrè AV, Sullivan TJ, Young TR, et al. The Genotype-Tissue Expression (GTEx) pilot analysis: Multitissue gene regulation in humans. Science. 2015;348:648–660.
23. Leppek K, Stoecklin G. An optimized streptavidin-binding RNA aptamer for purification of ribonucleoprotein complexes identifies novel ARE-binding proteins. Nucleic Acids Research. 2014;42:e13–e13.

Author names in bold designate shared co-first authorship.